Polymer Testing 135 (2024) 108465

Contents lists available at ScienceDirect

Polymer Testing

journal homepage: www.elsevier.com/locate/polytest

Poly(epoxy-imine) vitrimers. Effect of the structure on the stress relaxation and creep resistance

Tommaso Telatin [a], Silvia De la Flor [b], Àngels Serra [a,**], Xavier Montané [a,*]

[a] Universitat Rovira i Virgili, Department of Analytical and Organic Chemistry, C/ Marcel·lí Domingo 1, 43007, Tarragona, Spain
[b] Universitat Rovira i Virgili, Department of Mechanical Engineering, Av. Països Catalans 26, 43007, Tarragona, Spain

ARTICLE INFO

Keywords:
Vitrimers
Polyimines
Epoxy
Creep resistance
Stress-relaxation
Chemical degradation

ABSTRACT

A series of polyimine-epoxy vitrimers has been synthesized using commercially available monomers using a two-step synthetic route to maximize the content of imine groups in the resulting structures. The first step consists of the synthesis of amine terminated polyimine oligomers, which were synthesized by a condensation reaction of terephthalaldehyde (TA) with different proportions of diethylenetriamine (DETA) and a polyetheramine (Jeffamine D-230 or D-400). After that, the obtained viscous oligomers were cross-linked with bisphenol A diglycidyl ether (DGEBA). The design of network architectures using this approach is a powerful tool that allows controlling the concentration of imine groups, the dimensions of the intermediate polyimine oligomer and the polarity and mobility of its chains, confirming that it is an effective way to tune the thermal, mechanical and thermo-mechanical properties of the final materials. Furthermore, this work confirmed that an accurate design of the network architecture allows simultaneously improving the two main requirements of vitrimers by increasing the content of imine groups: fast stress relaxation processes and high creep resistance. Stress relaxation curves proved that these polyimine vitrimers could relax the 63 % of the initial stress in less than 9.6 min at 160 °C without any added catalyst. Besides, replacing Jeffamine D-400 with Jeffamine D-230 in the imine oligomer increases the material's resistance to creep at service temperatures. All the materials prepared present high thermal stability and showed T_gs between 31 and 93 °C.

1. Introduction

High mechanical performances and lack of recyclability and malleability are representative and inseparable binomials of thermosets. From this point of view, Covalent Adaptable Networks (CANs) could represent the key to unlocking these features and obtaining materials without compromising performance, processability, and environmental impact [1]. In particular, CANs are polymeric materials that exhibit a covalent tridimensional structure that, differing from common thermosets, can be triggered by applying a specific stimulus (for instance, temperature, light, solvent, pH) switching from a permanent to a dynamic network [2]. The dynamism of the network depends on the presence of chemical bonds that can undergo equilibrium reactions, determining a rearrangement of the 3D structure by cleavage of the existing bonds and forming new ones [3]. Without the proper stimuli, the process rate (i.e., the reaction rate) is very low, and the materials can be considered fully covalent, and their properties are comparable to a classic thermoset [4–6].

Based on the exchange mechanism, it is possible to divide CANs into two main categories. CANs in which the exchange reaction occurs stepwise, where the original bond first breaks and then the new bond is formed, are called dissociative. In contrast, CANs in which the exchange reaction occurs in a concerted way are called associative [7]. The nature of the exchange mechanism strongly affects the viscoelastic behavior of the material. It becomes evident by considering that a dissociative mechanism determines a drop in the cross-link density of the network when a stimulus is applied. However, the cross-link density can be considered constant in materials where the exchange reaction occurs through an associative path [5,6,8,9]. Consequently, the associative CANs exhibit a wide rubbery phase when heated over their glass transition temperature (Tg), while dissociative CANs are characterized by a solid-to-liquid transition [10]. Moreover, as first reported by Leibler et al., chemically associative CANs exhibit an Arrhenius-like dependence between viscosity and temperature, analogous to that of vitreous silica

* Corresponding author.
** Corresponding author.
E-mail addresses: angels.serra@urv.cat (À. Serra), xavier.montane@urv.cat (X. Montané).

https://doi.org/10.1016/j.polymertesting.2024.108465
Received 5 April 2024; Received in revised form 6 May 2024; Accepted 21 May 2024
Available online 22 May 2024

[11]. For this reason, they refer to these materials as vitrimers.

Several organic groups like disulfide bonds [12–14], esters [15–17], imines [18,19], boronic esters [20–22], vinylogous urethanes [23,24] and so forth, have been object of investigation as promising dynamic units for the synthesis of vitrimeric materials. Among them, imines represent an engaging chemical platform because of their reactivity and ease of synthesis by reacting aldehydes or ketones with primary amines in mild conditions. Imines are involved in three different equilibrium processes: Imine hydrolysis, transimination, and imine metathesis [25]. Transimination and imine metathesis occur even in the absence of a catalyst following a concerted mechanism and, for this reason, can determine the vitrimeric behavior of the material [26]. As demonstrated by Hu and coworkers, the imine hydrolysis reaction is catalyzed by acid and can be exploited for degradation purposes [27]. Two main strategies have been commonly adopted to produce polyimine vitrimers. The first one provides for the formation of the network directly by the reaction of a dialdehyde with a combination of a diamine and a triamine to obtain a fully polyimine network. Zhang and coworkers deeply investigated this kind of material [28–30]. Higher thermo-mechanical performance has been obtained using *m*-xylylene diamine and *m*-xylylene diamine dimer, thanks to the effects of conjugation structures in the network [31]. The second strategy involves the synthesis of an imine bond containing precursor that can be cured, as usually made in the production of traditional thermosets. In particular, the cited precursor can be a monomer containing imine groups, as synthesized by Zhao and coworkers from vanillin and 4,4′-methylenedianiline, using it as a curing agent for epoxidized soybean oil [32]. Besides, Roig and coworkers synthesized a diimine-diglycidyl monomer and then cured it with different polyether amines [33]. A different approach has been adopted by Liang and coworkers that prepared an imine containing NH_2-terminated linear prepolymer as the precursor and trimethyl citrate as cross-linker [34]. Through a similar strategy, Liu and coworkers obtained materials characterized by fast stress relaxations and superior tensile strength, Young modulus and thermal stability by using aromatic amines in the synthesis of the poly-imine curing agent and an off-stoichiometric ratio of curing agent and epoxy in the preparation of the materials [35].

Despite their promising properties, vitrimers have an Achilles' heel related to their susceptibility to creep under use conditions [36]. Although, even if at a temperature below the topological freezing temperature (Tv), the exchange reaction rate is low to the point that the exchange process can be considered negligible, many studies demonstrated that creep is also present in these conditions [37,38]. The introduction of permanent cross-links in a dynamic network represents a well-studied approach to suppressing creep. Torkelson and coworkers determined an upper limit for the proportion of permanent cross-links that is possible to introduce without compromising the dynamic properties of the material in terms of stress relaxation, degradability, and reprocessability [36]. Moreover, they developed a model that fits the experimental data and permits the prediction of the fraction of permanent cross-links that can be introduced. For fractions lower than this critical content, the formation of a fully permanent network that percolates the system cannot occur, and the overall dynamicity of the material is preserved. A kinetic modelling approach applied to CANs with different functionalities of the monomers, and the presence of permanent cross-links has been published recently by Konuray et al. [39]. This approach reveals great flexibility in the design of materials based on CANs with a broad range of vitrimer-like capabilities.

In the present work, our research aims are to develop an imine-based system capable of achieving rapid stress relaxation processes and high creep resistance by tuning the architecture and composition of the network. In view of all this, we have synthesized a series of polyimine-epoxy vitrimers starting from commercially available monomers as terephthalaldehyde (TA), diethylenetriamine (DETA), two different polyether amines (Jeffamine D-230 and D-400) that differ on the number of propylene oxide units, and bisphenol A diglycidyl ether (DGEBA). Jeffamines have been selected as amines since it is reported that polar groups enhance relaxation abilities in imines [40]. We report a procedure in which amine-terminated polyimine oligomers are synthesized by the reaction of TA with different combinations of DETA and Jeffamine D-230 or D-400. Then, the obtained linear oligomers were cross-linked by reaction with a stoichiometric amount of DGEBA. The thermal stability of the polyimine-epoxy vitrimers was evaluated by thermogravimetry, and the thermomechanical properties and vitrimeric behavior by dynamic mechanical thermal analysis (DMTA). Chemical degradation has also been tested, revealing that almost full degradation could be reached by tuning the material composition. In this sense, the novelty of this approach has been to report that by using this methodology, we can tailor the concentration of imine groups in the final networks, which in turn defines the vitrimeric behavior, thermomechanical characteristics and creep resistance.

2. Materials and methods

2.1. Materials

The following chemicals were purchased from Sigma-Aldrich: diethylenetriamine (DETA, 99 %), poly(propylene glycol) bis(2-aminopropyl ether) (Jeffamine D-230, $M_{\bar{n}}$230 g/mol), terephthalaldehyde (TA, 99 %). Bisphenol A diglycidyl ether (DGEBA, trade name ARALDITE GY240, 5.51 eq/kg) and poly(propylene glycol) bis(2-aminopropyl ether) (Jeffamine D-400, $M_{\bar{n}}$430 g/mol) were purchased from Huntsman. 2-Propanol (*i*-PrOH) was purchased from Carlo Erba, and tetrahydrofuran (THF) from Scharlau. All chemicals were used as received.

2.2. General procedure for the synthesis of polyimine oligomers

A typical procedure for the synthesis of polyimine oligomers is the following. In a round bottom flask equipped with a magnetic stirrer and reflux condenser, the corresponding amounts of TA, DETA and Jeffamine D-230 (or D-400) were dissolved in a mixture of THF and *i*-ProH (3/1 v/v). The reaction mixture was magnetically stirred and maintained at 60 °C for 2 h. After that, the mixture of solvents was eliminated in the rotary evaporator, and the samples were dried under vacuum at 80 °C for 24 h. The oligomers are coded as "*X a/b y%*", where *X* refers to the Jeffamine used in the synthesis (D-230 or D-400), *a* indicates the percentage in mol of DETA, while *b* is the % in mols of Jeffamine. Finally, *y* corresponds to the excess of amine used in the synthesis calculated using the following formula:

$$y = \left(\frac{eq_{NH_2}}{eq_{CHO}} - 1\right)\cdot 100 \qquad \text{(Equation 1)}$$

where eq_{NH_2} is the number of equivalents of $–NH_2$ groups and eq_{CHO} is the number of equivalents of aldehyde groups. For example, the code D230 50/50 40 % refers to an oligomer synthesized using an equimolar amount of DETA and Jeffamine D-230, with a 40 % mol excess of total amine in the reaction. Table 1 details the composition in mols of each compound used in the synthesis of the oligomers.

2.3. General procedure for the preparation of vitrimeric samples

The polyimine-epoxy vitrimers were obtained according to the following procedure. In a glass vial, the polyimine oligomer was mixed with DGEBA in stoichiometric proportions (Table 1). Then, the mixture was degassed under vacuum at 40 °C and poured into a rectangular Teflon mold of 30 x 5 × 1.5 mm^3. The samples were cured in an oven using the following schedule: 3 h at 100 °C, 2 h at 150 °C, and 2 h at 180 °C. The cured materials are coded by adding "C" at the end of the corresponding oligomer code.

Table 1
Composition of the oligomers and the mixtures, molecular parameters and rheological data obtained for all the formulations.

Sample	TA (mmol)	DETA (mmol)	D230 (mmol)	D400 (mmol)	Excess of amine[a] (% mol)	DGEBA (meq.)	Theoretical M_n (g/mol)	[Imine] [b] (meq/g)	[PPO] [c] (meq/g)	η [d] (Pa·s)	t_{gel} [e] (s)
D230 50/50 40%-C	8.50	5.95	5.95	–	40	19.54	1982	2.67	2.23	27.33	380
D230 25/75 40%-C	8.50	2.98	8.93	–	40	16.57	2280	2.74	3.43	13.30	813
D230 50/50 15%-C	8.50	4.89	4.89	–	15	9.99	4319	3.98	2.67	171.93	136
D230 25/75 15%-C	8.50	2.44	7.33	–	15	7.54	4942	4.11	4.12	255.12	1355
D400 50/50 40%-C	8.50	5.95	–	5.95	40	19.54	2782	2.25	4.62	10.23	896
D400 25/75 40%-C	8.50	2.98	–	8.93	40	16.57	3480	2.13	6.57	9.04	2029
D400 50/50 15%-C	8.50	4.89	–	4.89	15	9.99	5954	3.24	5.36	279.69	909

[a] Excess of amine used in the synthesis of the polyimine oligomers with respect to aldehyde.
[b] Theoretical concentration of imine groups in the cured materials.
[c] Theoretical concentration of polypropylene oxide units in the cured materials.
[d] Viscosity of the formulations, as prepared, measured at 30 °C.
[e] Gel time of the formulations measured at 100 °C.

2.4. Characterization techniques

^{1}H NMR and ^{13}C NMR spectra were recorded in a Varian VNMR-S400 NMR spectrometer. $CDCl_3$ was used as the solvent. All chemical shifts are quoted on the δ scale in part per million (ppm) using residual protonated solvent signal as the internal standard (^{1}H NMR: $CDCl_3 = 7.26$ ppm; ^{13}C NMR: $CDCl_3 = 77.16$ ppm).

The viscosity of each formulation was measured using an ARES-G2 rheometer (TA Instruments) equipped with an electrically heated plate device (EHP) and parallel plate geometry. Each sample was conditioned at 30 °C for 3 min. Experiments were conducted applying a scan of shear rate between 0.1 s^{-1} and 10 s^{-1} and sampling the value of the stress 5 times per decade. The viscosity (η) of the mixture was calculated by interpolating the obtained data using the following equation:

$$\tau = \eta\dot{\gamma} \quad \text{(Equation 2)}$$

where τ is the stress, $\dot{\gamma}$ is the shear rate, and η is the viscosity, which is given by the slope of the linear relationship between τ and $\dot{\gamma}$.

The gelation during curing was evaluated with the same instrument. For these samples, dynamic tests at a frequency of 1 Hz, with 0.1 % oscillation strain were performed to investigate the evolution of the storage and loss modulus (G' and G'' respectively). The experimental procedure was defined to simulate the curing reaction in the oven at 100 °C for 3 h. The gelation time was identified as the time at which the crossover of the G' and G'' curves occurred.

The thermal stability of the materials was evaluated using a Mettler Toledo TGA 2 thermobalance. Cured samples weighing around 10 mg were degraded between 30 and 600 °C at a heating rate of 10 °C min^{-1} in N_2 atmosphere with a flow rate of 50 cm^3 min^{-1}.

The thermomechanical properties were studied using a DMTA Q800 (TA Instruments) equipped with a film tension clamp. Prismatic rectangular samples with dimensions of around 30 x 5 × 1.5 mm^3 were analyzed from −10 to 180 °C at 1 Hz, with 0.1 % strain at a heating rate of 2 °C min^{-1}. Tensile stress-relaxation tests were conducted in the same instrument using the film tension clamp on samples with the same dimensions as previously defined. The samples were first equilibrated at the relaxation temperature for 5 min, and a constant strain of 1 % was applied, measuring the consequent stress level as a function of time. The materials were tested only once at one temperature. The relaxation-stress σ(t) was normalized by the initial stress σ_0, and the relaxation times (t^*) were determined as the time necessary to relax $0.37\sigma_0$, (i.e., $\sigma = 1/e\sigma_0$). With the relaxation times obtained at each temperature, the activation energy values (E_a) were calculated using an Arrhenius-type equation:

$$ln(t^*) = \frac{E_a}{RT} - ln(A) \quad \text{(Equation 3)}$$

where t^* is the time needed to attain a given stress-relaxation value ($0.37\sigma_0$), A is the pre-exponential factor, T is the absolute temperature, and R is the universal gas constant.

Creep tests were conducted in the same DMTA Q800 instrument. The sample was equilibrated at 20 °C for 5 min, after which the stress (σ) was applied for 30 min and then released. The strain (ε) was measured as a function of time during the application of the stress and for an additional 30 min for the stress recovery. The applied stress was chosen ensuring that each material was in its viscoelastic range. The temperature of 20 °C was chosen as representative of common service condition.

The chemical degradation of the vitrimeric materials was conducted by first weighing the sample of the cured material and then soaking the sample in a 1 M HCl and THF solution (2/8 v/v) for 72 h at 50 °C under stirring. Then, the solutions were filtered, and the residues were washed with acetone and dried at 100 °C until they reached constant weight. The mass of the dried residue (%r) was calculated in terms of percentage as follows:

$$\%r = \frac{m_r}{m_0}100 \quad \text{(Equation 4)}$$

where m_r is the mass of the dried residue, and m_0 is the initial sample mass.

3. Results and discussion

3.1. Synthesis of the polyimine oligomers

Polyimine oligomers were synthesized by condensation reaction of terephthalaldehyde (TA) with diethylenetriamine (DETA) and either Jeffamine D-230 or D-400 at 60 °C for 2 h in a mixture of THF and 2-propanol (3/1 v/v) (Scheme 1). The composition of the mixtures is given in Table 1. Setting out stoichiometric reaction conditions is fundamental to ensure the formation of oligomers with the required end groups. Specifically, the syntheses were carried out using an excess of amine to promote the formation of amine-terminated telechelic oligomers with imine groups along the chains.

The oligomers were characterized by NMR spectroscopy. Fig. S1 shows the ^{1}H NMR spectrum of D230 50/50 40 % in $CDCl_3$, which presents broad signals in the aliphatic region between 0.8 and 4.2 ppm.

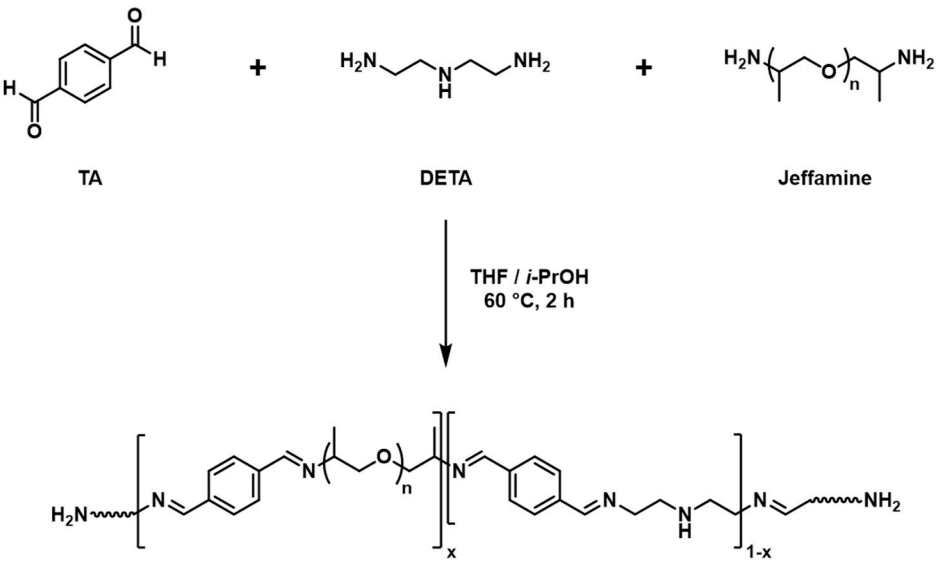

Scheme 1. General scheme of the synthesis of polyimine oligomers.

This corroborates the formation of macromolecular structures.

In addition to the aromatic protons of the TA unit, a complex peak centered at 8.23 ppm appears. This peak corresponds to the imine protons from the condensation of the primary amines with the aldehyde, which can be affected by the cis/trans isomerism. The total absence of the aldehyde protons (expected at 10.4 ppm) confirms that the reaction has been completed and that the telechelic oligomer has only amines as end-groups.

Due to the high complexity of the oligomers with a copolymeric structure, we prepared the corresponding homooligomers for both amines and recorded the ^{13}C NMR spectra (Figs. S2 and S3). With these data, we could assign most of the signals that appear in the spectra of the copolymeric oligomer.

Fig. 1 shows the ^{13}C NMR spectrum of the oligomer D230 50/50 40 % with the corresponding assignments. First of all, the signals at 161.6 and 161.2 ppm are attributed to the imine carbons formed by the reaction of DETA and TA (indexed as 5 and 5′, for terminal and central imine units, respectively) while the signal at 159.9 ppm belongs to imine carbons originated by the reaction of Jeffamine and TA (11 and 11'). The peaks between 143.3 and 128.0 ppm are related to the aromatic carbons of the TA units.

Moving upfield in the spectrum, the region between 78.2 and 72.6 ppm includes the signals belonging to the carbons of the polypropylene oxide (PPO) chain of the Jeffamine units overlapped with the deuterated solvent. Moreover, the signal observed at 66.2 ppm confirms that the reaction between Jeffamine and TA took place since it is assigned to the tertiary carbon of the PPO chain contiguous to the nitrogen of an imine group in the resulting structure (**10** and **10'**). At 46.4 ppm, the signal of the same tertiary carbon contiguous to –NH_2 terminal groups (**6**) is still visible due to the excess of amine added.

Regarding DETA units, two signals can be attributed to the carbons bonded to nitrogen of the formed imine groups. These signals, which appear at 55.9 and 53.4 ppm (**4** and **4′**), are associated with an imine group DETA at the end chain and double condensed DETA, respectively. Analogously, the methylene carbon contiguous to the secondary amine next to carbon **4** (**3** and **3'**) can be observed at 49.8 and 48.4 ppm, respectively. The peaks at 44.9 ppm and 41.7 ppm are related to the methylene carbons contiguous to the primary amine and secondary amine of DETA end groups (**2** and **1**). The low intensity of signal **1** could indicate that DETA is mainly located in the central units of the oligomer chains, which means that both primary amine groups of DETA have reacted with TA. The presence of unreacted primary amine as end-groups from both DETA and Jeffamine units in the spectrum indicates

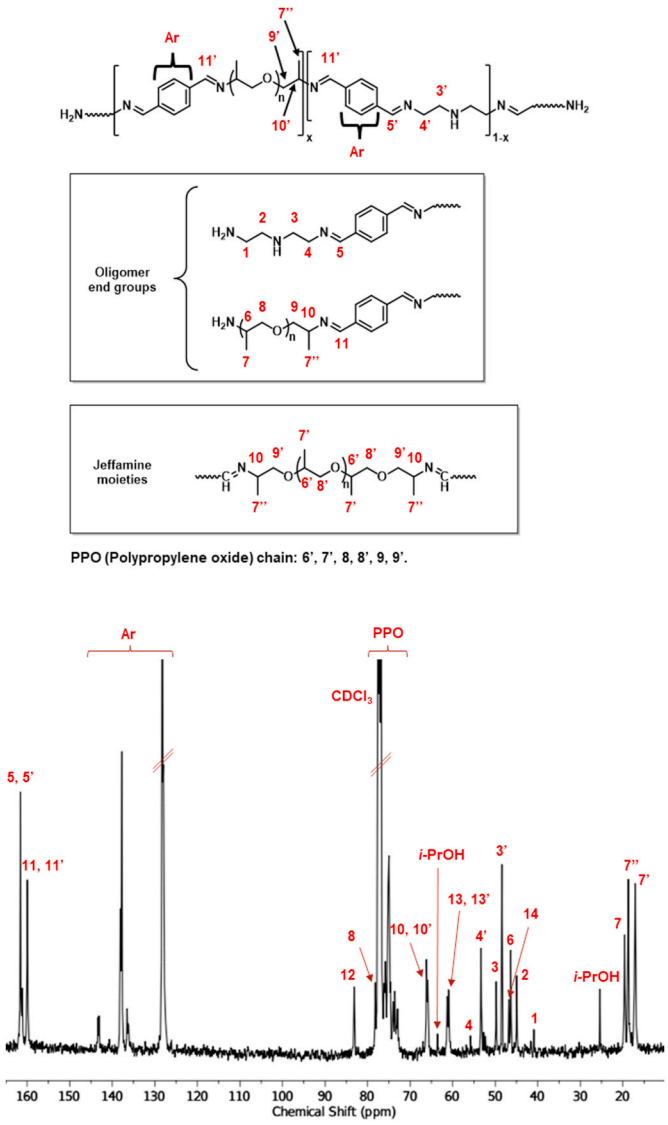

Fig. 1. ^{13}C NMR spectrum of the oligomer D230 50/50 40 % in $CDCl_3$.

that the oligomer predominantly exhibits a random sequence.

The peaks observed at 83.2, 61.2, 61.0 and 46.8 ppm belong to the carbons of the imidazolidine structure formed by the nucleophilic attack of the secondary amine present in the DETA units to the intermediate carbinolamine instead of the generation of the expected imine (Scheme S1) [41].

Finally, three peaks between 19.6 and 17.1 ppm are assigned to the methyl carbons of the Jeffamine (**7, 7′** and **7″**). The methyl group near an amine end group appears at 19.6 ppm (**7**). The peak at 18.7 ppm (**7″**) is assigned to the methyl close to the inner imine groups, while the peak at 17.1 ppm (**7'**) is attributed to the methyl carbons of the PPO repetitive unit.

Moreover, the extent of the excess amine added is crucial for the final number average molecular weight (M_n) of the oligomer, which can be estimated by first calculating the degree of polymerization using the following equation [42]:

$$DP_n = \frac{r+1}{2r(1-p)+(1-r)} \quad \text{(Equation 5)}$$

where DP_n is the number-average degree of polymerization, r is determined by the following quotient: $r = \frac{N_{CHO}}{N_{amine}}$, where N_{CHO} is the number of moles of aldehyde, N_{amine} is the total number of mols of amine, and p is the extent of the reaction, considered equal to 1 when the reaction is completed.

The theoretical M_n is then calculated by using the next equation:

$$M_n = 2M_e + DP_n M_r \quad \text{(Equation 6)}$$

where M_e is the average molecular weight of the end groups of the oligomer, and M_r is the average molecular weight of the repeating units. It is essential to underline that this theoretical estimation of the M_n considers the proportion of each amine in the monomers' mixture. Variations associated with the reactivity of the monomers are not considered.

Observing the values of the M_n calculated for each oligomer (Table 1), it is possible to note a slight increase in the molecular weight when increasing the proportion of Jeffamine to the proportion of DETA from 50 to 75 % mol. On the other hand, reducing the excess of amine employed in the synthesis of the oligomers from 40 to 15 % causes a more pronounced increase of the M_n.

3.2. Study of the curing procedure

The prepared oligomers were used stoichiometrically as hardeners for DGEBA. The molecular parameters and rheological data of the analyzed samples are presented in Table 1. The concentration of imine and PPO groups was determined for each formulation. The viscosity of the initial formulation of polyimine oligomer and DGEBA was investigated at 30 °C following the evolution of the shear stress as a function of the shear rate for all the compositions (Fig. S4). This temperature was chosen on the assumption that it is the lower limit in the liquid molding processes commonly used in the manufacture of thermosets. As expected, the viscosity of the mixtures is strongly affected by the molecular weight of the polyimine oligomers, with formulations prepared with the highest molecular weight oligomers exhibiting the highest viscosity values.

The determination of gel time is crucial when curing the formulations from both scientific and technological points of view. The time needed to reach the gel point for each formulation was determined by curing at 100 °C, as it is done in the oven, in a rheological oscillatory shear test. The gel time values in Table 1 show that gelation is already reached during the curing process at 100 °C in less than 35 min. Notably, a reduction in the proportion of DETA leads to longer gelation times. This is evident when comparing 25/75 with 50/50 formulations. The presence of secondary amine groups in the DETA moieties can easily explain this tendency, considering that they can also react with DGEBA, increasing the amine functionality and forming a more cross-linked network.

Regarding the reaction of the $–NH_2$ end groups of the polyimine oligomer with DGEBA, it must be considered that the stoichiometry of the reaction is equal to 2:1 in terms of equivalents of $–NH_2$ and epoxy groups, respectively. On the other side, the secondary amines of DETA units in the oligomer react with a stoichiometry equal to 1:1 with epoxy groups. In light of this, the ring-opening addition of amine to the epoxy ring determines the formation of linear permanently bonded chains, where the reaction of DGEBA with a primary amine is responsible for the growth of the chain, while the reaction with a secondary amine from a DETA unit determines the interruption of the chain elongation. Therefore, as schematically illustrated in Fig. 2, the cured material can be depicted as composed of covalent non-dynamic chains linked to each other by dynamic polyimine chains. The network architecture obtained is directly related to the synthetic strategy employed to obtain the materials.

3.3. Thermal stability of the materials

The thermal stability of the vitrimeric materials was determined by thermogravimetry. Table 2 presents the most significant data extracted from TGA curves, and Fig. S5 shows the TGA curves and their derivatives for the prepared materials. DTGA curves show that thermal degradation occurs via two-step weight loss with a similar stability pattern. The resulting vitrimers are stable up to 269 °C, the lower temperature at which a loss of 1 % of the weight was detected. These results ensure safe reprocessability until 220 °C. Furthermore, replacing Jeffamine D-230 with Jeffamine D-400 reduces the final char yield of the vitrimer.

3.4. Thermomechanical characterization of the materials

The thermomechanical properties of the materials were investigated by DMTA. Fig. 3 shows the evolution of storage modulus and loss tangent (tan δ) with temperature for all the prepared materials and Table 2 collects the most characteristic data. Furthermore, Fig. S6 shows the plot of loss modulus against the temperature for all the materials.

First of all, it was observed that the storage modulus E' in the glassy and in the rubbery states and the position of the tan δ peak ($T_{g\text{-}tan\ \delta}$) vary considerably depending on the sample analyzed, confirming the fine tunability of the system. The different proportions of Jeffamine used, as well as its polyether chain length, determine the flexibility of the polymer chains and the thermomechanical properties of the resulting networks.

By comparing the $T_{g\text{-}tan\ \delta}$ values with the concentration of PPO units, it is observed that an expected increase in mobility caused by the introduction of a higher proportion of polyether units (either by adding a longer Jeffamine or a larger amount of this diamine) affects the short-range molecular motion associated with the glass transition reducing the $T_{g\text{-}tan\ \delta}$ (Fig. 4a). In other words, an increase in the content of PPO units leads to a decrease in the cross-linking density since these units act as spacers between the cross-linking points. A similar correlation is found between the concentration of PPO units and the storage modulus in the rubbery state (Fig. 4b). This result agrees with the well-known relationship existing between $E'_{rubbery}$ and the cross-link density of the material [2]:

$$d = \frac{E'_{Rubbery}}{3R\left(T_{g\text{-}tan\ \delta}+40\right)}10^6 \quad \text{(Equation 7)}$$

where d is the cross-linking density, $E'_{Rubbery}$ is the storage modulus in the rubbery state (in Pa), R is the gas constant, and $T_{g\text{-}tan\ \delta}$ is the temperature of the maximum of the tan δ curve.

Regarding the storage modulus in the glassy state (E'_{Glassy}), it is observed that it varies significantly (1662–2672 MPa) in the prepared materials. No linear correlation was found with any specific parameter

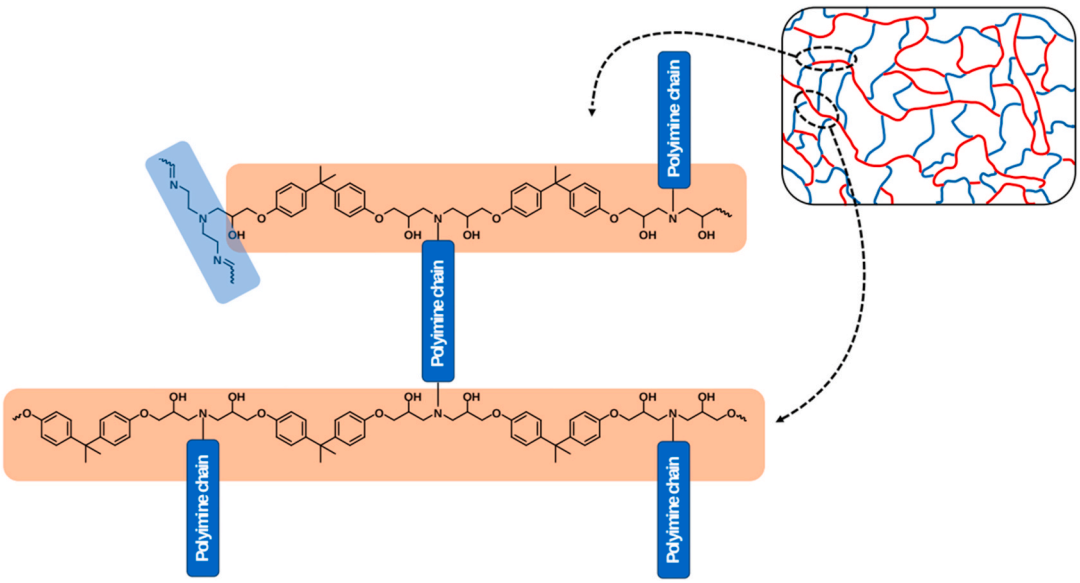

Fig. 2. Schematic illustration of the network architecture. Red lines represent the permanent linear chains while blue lines represent the dynamic polyimine-based chains. (For interpretation of the references to colour in this figure legend, the reader is referred to the Web version of this article.)

Table 2
Thermal and creep resistance, thermomechanical and vitrimeric properties of the prepared materials.

Sample	$T_{1\%}$ [a] (°C)	Char Yield [b] (%)	$T_{g\text{-tan }\delta}$ [c] (°C)	E'_{Glassy} [d] (MPa)	$E'_{Rubbery}$ [e] (MPa)	Cross-link density [f] (mol/m^3)	t* [g] (min)	E_a (kJ/mol)	T_v [h] (°C)	dε/dt [i]	% Residual deformation [j]
D230 50/50 40%-C	269	21.3	93.2	1662	19	1812	7.0	85 ± 10	86 ± 7	$6.8{\cdot}10^{-3}$	0.51
D230 25/75 40%-C	278	25.0	87.7	1854	14	974	4.8	55 ± 6	46 ± 10	$11.1{\cdot}10^{-3}$	0.46
D230 50/50 15%-C	274	28.0	80.6	2181	18	1762	4.4	51 ± 9	40 ± 15	$6.9{\cdot}10^{-3}$	0.19
D230 25/75 15%-C	272	29.3	60.0	2485	9	967	1.2	33 ± 1	−31 ± 4	$7.2{\cdot}10^{-3}$	0.14
D400 50/50 40%-C	279	18.3	55.3	1910	13	1152	9.6	60 ± 10	62 ± 12	$37.1{\cdot}10^{-3}$	0.84
D400 25/75 40%-C	269	19.1	31.4	2672	7	845	1.4	28 ± 5	−53 ± 14	$34.9{\cdot}10^{-3}$	0.85
D400 50/50 15%-C	276	24.5	45.2	2616	11	1191	1.8	46 ± 10	10 ± 17	$118.9{\cdot}10^{-3}$	1.86

[a] Temperature of 1 % of weight loss.
[b] Char residue at 600 °C.
[c] Temperature at the maximum of tan δ peak at 1 Hz.
[d] Storage modulus in the glassy state (at $Tg\text{-}_{tan\ \delta}$ - 50 °C).
[e] Storage modulus in the rubbery state (at Tg-tan $_{\delta}$ + 50 °C).
[f] Cross-link density calculated from the storage modulus in the rubbery state.
[g] Time to reach a value of $\sigma/\sigma_0 = 0.37$ at 160 °C except D400 25/75 40%-C, which has been measured at 150 °C.
[h] Topology freezing temperature obtained from the Arrhenius relationship.
[i] Determined from the slope of the steady-state region of the creep curve.[j] Determined after 30 min of releasing the stress.

of the system, suggesting that these macroscopic properties are the result of a combinatorial effect of more than one microscopic event. For example, the imine groups, PPO units, and hydroxyl groups formed by the ring-opening reaction of the oxirane groups during the curing contribute to increasing the polarity of the polymer chains and to the formation of hydrogen bonds and, consequently, the intermolecular interactions that affect E'_{Glassy}.

3.5. Study of the vitrimeric behavior

The polymer networks have imine bonds that can undergo equilibrium exchange reactions. Therefore, these networks are expected to rearrange above a certain temperature toward a relaxed structure when mechanical stress is applied, determining an attenuation of the stress response.

The kinetics of an exchange reaction in a polymeric matrix can be rationalized with the same criteria applied to a reaction that occurs in a condensed phase, for instance, in solution. At a given temperature, the reaction rate depends on the concentration of the reagents, considering that it affects the frequency of collisions by which the bimolecular events of the reaction take place. The efficiency of these events depends on the activation energy of the reaction that, in turn, is strongly influenced by the solvent. In the same way, it can be assumed that the network architecture and its composition affect the activation energy of the exchange process in a vitrimeric material. Moreover, the vitrimeric matrix can be considered as a condensed phase over the T_g, characterized by very high viscosity. Therefore, the mobility of the moieties involved in the exchange reaction becomes decisive for the overall process rate in the same way as diffusive processes are in solution [43].

In this specific work, the stoichiometric reaction of the polyimine

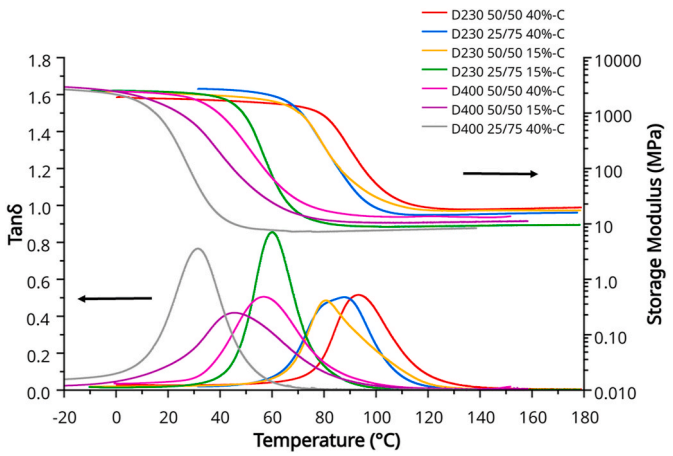

Fig. 3. Evolution of storage modulus and tan δ with temperature for all the materials.

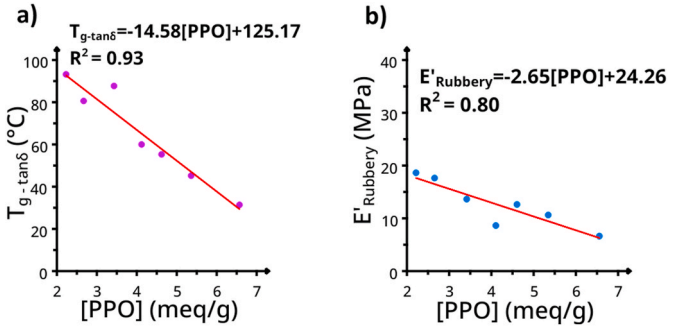

Fig. 4. Correlation between: a) $T_{g\text{-}tan\ \delta}$ and concentration of PPO units; b) $E'_{Rubbery}$ with the concentration of PPO units.

oligomer with DGEBA during the curing process ensures that the exchange process is associated with imine metathesis reactions since no free amines are present. The vitrimeric properties of the prepared materials have been investigated by DMTA. Stress relaxation experiments were performed at different temperatures above the T_g (i.e. $T_{g\text{-}tan\ \delta}$) for all the prepared materials. The resulting stress relaxation curves for each material are shown in Fig. 5 (materials prepared with Jeffamine D-230) and Fig. S7 (materials prepared with Jeffamine D-400), while the main data extracted are summarized in Table 2.

It should be noted in the figures that the relaxation curves for the different materials are recorded in different temperature ranges because their T_gs are different, and the stress relaxation analysis has to be performed in the rubbery region. The curves show the rapid relaxation of these materials as they reach the reference relaxation value (0.37 $\sigma/\sigma_0 =$ 1/e) in a few minutes at 160 °C, and for some materials, even at lower temperatures.

The stress-relaxation capabilities of the prepared materials were firstly analyzed by representing the relaxation curves with stretched exponential functions in accordance with the Kohlrausch−Williams−-Watts (KWW) model. The obtained stretching parameters resulted close to 1, confirming that the experimental data fit well to the simpler Maxwell model. Thus, the Arrhenius plot was then constructed, representing the times necessary to reach 0.37 σ/σ_0 against the inverse absolute temperature, including the confidence intervals for the linear regression adjustment (Fig. S8 and Table S1). As expected, the calculated E_as (Table 2) were found to decrease by increasing the

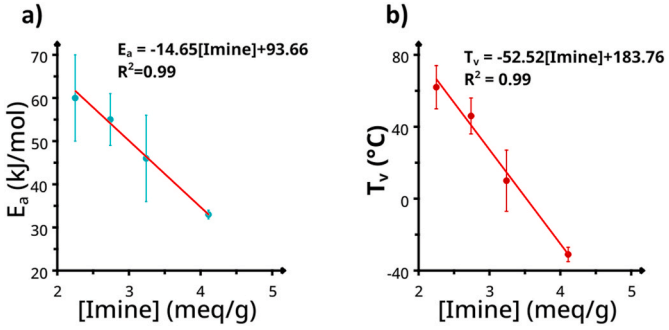

Fig. 6. Correlation between: a) E_a and imine concentration; and b) T_v and imine concentration.

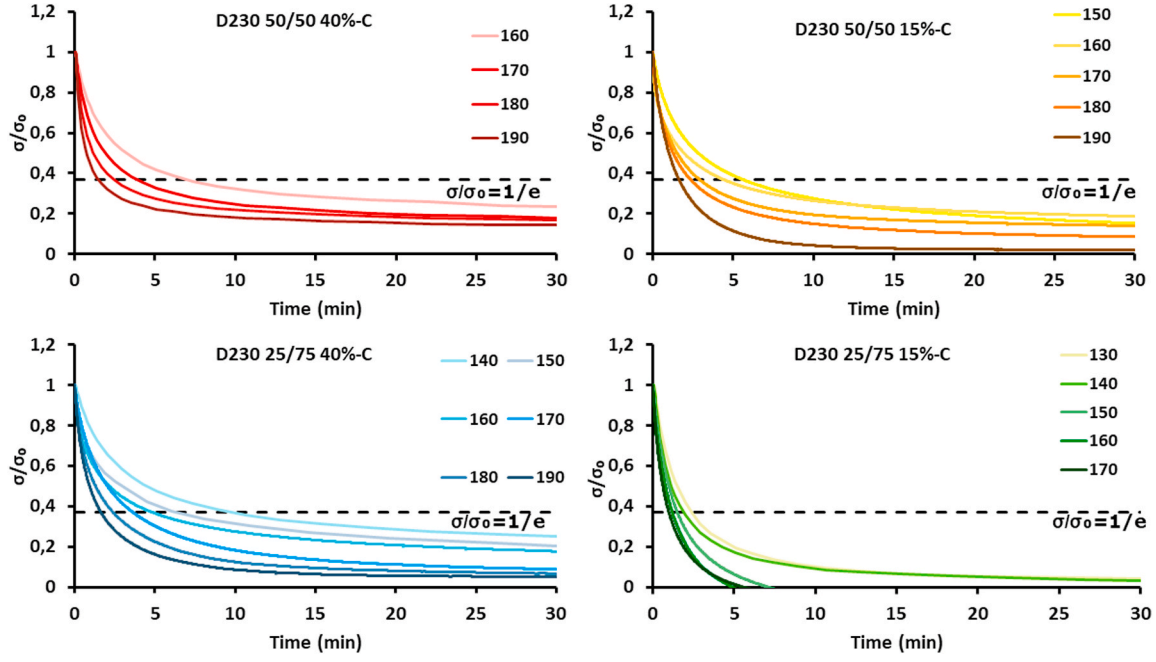

Fig. 5. Normalized stress relaxation curves as a function of time for the materials prepared with Jeffamine D-230 at different temperatures.

concentration of exchangeable imine groups when the cross-linking density was kept almost constant (Fig. 6a).

According to the Arrhenius equation, the topology freezing temperature (T_v) was also calculated. T_v is defined as the temperature at which the material reaches a viscosity of 10^{12} Pa s, and it is considered the temperature at which chemical interchanges start to occur. However, if T_v is lower than T_g, the vitrimeric exchange only occurs when T_g is overpassed, and the chains of the network have sufficient mobility to interact with each other.

As observed for E_a, T_v also exhibits a linear decrease with increasing the concentration of imine groups (Fig. 6b). It is reasonable to assume that, as mentioned above, the exchange process can be considered as a common chemical reaction, and therefore, an increase in the reagents' concentration implies an increase in the frequency of the molecular collisions through which the reaction takes place. These observations are in agreement with the results reported by Miao and co-workers [44], who investigated the relationship between the content of exchangeable groups and the dynamic behavior in *trans*-carbamoylation-based vitrimers. Thus, the linear dependence of E_a and T_v on the concentration of dynamic groups is still valid in the present imine-based vitrimeric systems, which also have the advantage that the dynamic change can be tuned simply by modulating the molecular weight of the telechelic oligomer.

3.6. Creep resistance

Creep recovery experiments were performed to evaluate the viscoelastic response of all the vitrimers at 20 °C. The resulting normalized strain *vs.* time curves are shown in Fig. 7 while the creep rate and the residual deformation of all the tested materials are collected in Table 2.

Fig. 7 shows that samples prepared with Jeffamine D-230 exhibit good creep resistance at 20 °C, while the creep deformation is higher in samples prepared with Jeffamine D-400. Thus, the use of a polyetheramine with a shorter PPO chain, such as Jeffamine D-230, can improve the creep resistance. The extremely low creep resistance of samples D400 25/75 40%-C and D400 50/50 15%-C compared to the other sample prepared with this Jeffamine can be attributed to their loss modulus values, which at 20 °C are very close to their maximum (Fig. S6). However, the material shows a consistent strain recovery upon stress relief, as expected for a viscoelastic recovery process, with a residual normalized strain after 30 min of stress relief of 0.849 and 1.864, respectively. This behavior is categorized as primary creep [45] since the presence of a high amount of PPO units in the network increases the mobility of the chains and, consequently, their conformational freedom. The tendency of these samples to recover the strain after the release of the stress demonstrates that the imine metathesis is negligible at 20 °C. Therefore, in the absence of external stimuli, the network returns to the initial conformation.

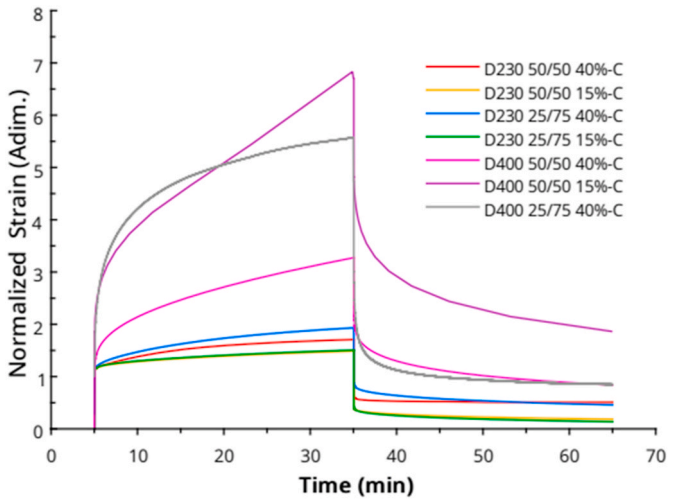

Fig. 7. Creep experiments at 20 °C for all the prepared materials.

Moreover, sample D400 50/50 40%-C, in which the proportion of Jeffamine D-400 is the lowest of this family of samples, but the concentration of imine groups is similar to that of sample D400 25/75 40%-C, exhibited a lower total creep deformation but a similar secondary creep. It confirms that in these systems, the high content of PPO units has a relevant impact on the primary creep, which is the main responsible of their creep behavior. On the other hand, the creep rates, which can be considered proportional to the inverse of the materials' viscosities, are similar for these two materials according to the comparable content of imine groups, whose reactivity determines the emergence of vitrimers fluid-like behavior. The extremely high creep rate of sample D400 50/50 15%-C is due to the loss modulus of the material, which is at its maximum value at the temperature tested (20 °C). From this point of view, the effect of any exchange reactions involving the imine groups of the material is negligible.

On the other hand, samples prepared with Jeffamine D-230 do not show significant differences in creep resistance. The concentration of the aromatic imine moieties influences the creep behavior. Comparing the samples D230 50/50 40%-C and D230 50/50 15%-C, which have a concentration of imine groups equal to 2.549 meq/g and 3.711 meq/g, respectively, it is observed that the higher the content of rigid imine groups the lower the primary creep and the higher the strain recovery. This could be attributed to the high rigidity that imines impart to the polymer chains and the consequent low conformational freedom. It would be expected that as the proportion of Jeffamine increases, the creep deformation would also be much more significant. However, sample D230 50/50 40%-C does not follow the expected behavior and shows a slightly higher primary creep than D230 25/75 15%-C. This could be attributed to the lower proportion of imine moieties and the resulting less rigid network structure. In fact, primary creep is also the main reason for the different behavior of these two materials in this case. In contrast, the different concentration of imine groups does not affect the creep rate, indicating that exchange reactions are negligible at 20 °C for these systems. Finally, D230 25/75 40%-C differs from the other D-230-based samples, exhibiting a slightly higher primary creep due to the higher content of PPO units. Thus, in general, a reduction in the creep at 20 °C can be observed as the PPO content decreases and the concentration of imine moieties increases.

However, the negligible rate of the imine metathesis reaction at 20 °C is determined by the higher T_g values of the prepared materials. As mentioned before, T_v is lower than T_g, for all the materials except D400 50/50 40%-C, and therefore T_g represents the temperature limit below which the chains of the network have not enough mobility to interact with each other. Consequently, at a temperature lower than the glass transition temperature imine metathesis reaction does not affect the mechanical properties of the materials and the creep behavior is only attributable to the loss modulus.

3.7. Chemical degradation

It is known that imine bonds can be hydrolyzed under acidic conditions. In this study, the chemical degradability of the polyimine-based vitrimers was investigated at 50 °C for 72 h using a mixture of 1 M HCl and THF (2/8 v/v). The combination of the acid solution with an organic solvent has a synergistic effect that facilitates the penetration of the H_3O^+ into the cross-linked network since, in this case, THF increases the wettability of the polymer surface, favoring its erosion by the hydrochloric acid [46]. The results obtained during the chemical degradation tests for all the vitrimeric materials are shown in Fig. 8 and summarized in Table S2. As illustrated in Fig. 2, these networks are composed of linear epoxy chains bonded to a dynamic structure. Therefore, higher degrees of degradation were expected for all the samples. Nevertheless, the lower chemical degradability observed for many of the samples

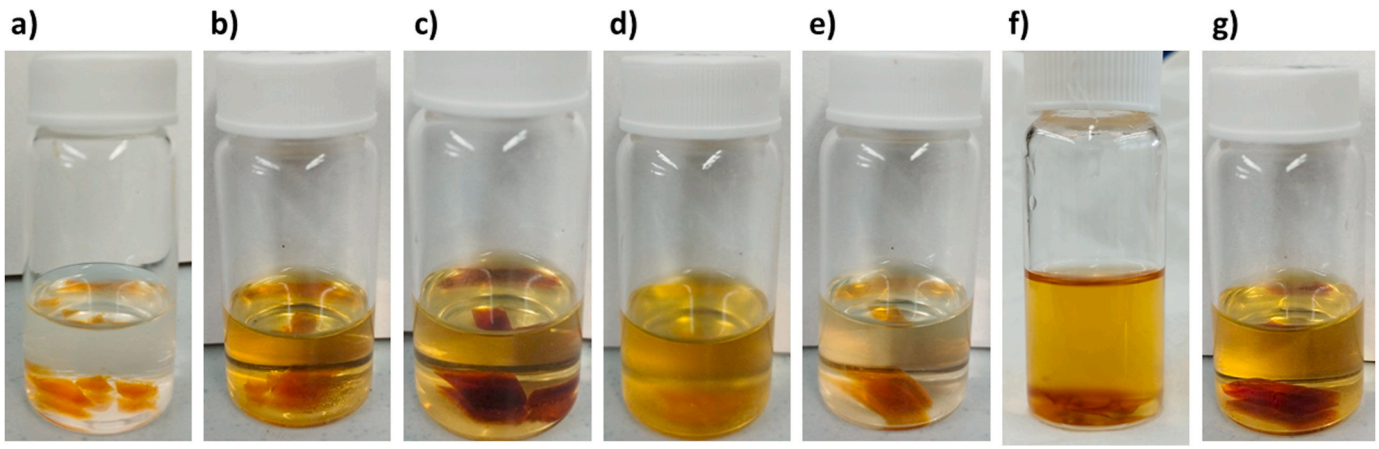

Fig. 8. Chemical degradation of all the prepared vitrimers: a) D230 50/50 40%-C; b) D230 25/75 40%-C; c) D230 50/50 15%-C; d) D230 25/75 15%-C; e) D400 50/50 40%-C; f) D400 25/75 40%-C; and g) D400 50/50 15%-C.

could be related to several reasons: a) Segregation of DETA units mainly in the central part of the oligomer chains compared to Jeffamine due to their different reaction rate with the dialdehyde, which could imply that highly cross-linked microdomains are formed by the reaction of secondary amines with DGEBA. Besides, these microdomains are characterized by a very tight tridimensional structure that is impenetrable by the acidic solution, and b) Length of the oligomer, which correlates with the length and the amount of the Jeffamine used. From the values in the table, it can be seen that the lower the molecular weight of the Jeffamine and the lower the amount of this diamine we use, the less the material degrades. As evidence of this fact, the sample D230 50/50 40%-C practically does not degrade. Besides, the low polarity of these materials is responsible for the poor accessibility of the acidic mixture within the tridimensional structure of the vitrimers. When more polar solvents such as dimethyl formamide were used, the degradation could not be improved because a permanent network was still present in the solution despite the hydrolysis of the imine bonds.

4. Conclusions

A series of polyimine-epoxy vitrimers were synthesized by a two-step procedure. First, an amine-terminated oligomer was prepared by a condensation reaction of terephthalaldehyde with diethylenetriamine and Jeffamine D-230 or D-400 in different proportions. These oligomers were characterized by NMR spectroscopy. This methodology allowed us to build up well-defined oligomers with known imine groups.

The oligomers were further reacted with DGEBA to obtain a cross-linked network. The resulting materials exhibited a high thermal stability with an initial degradation temperature above 260 °C. This stability allows safe reprocessing of the polyimine vitrimers.

Thermomechanical properties, such as E' and $T_{g\text{-}tan\ \delta}$, were found to be directly correlated with the content of PPO units in the network opening the possibility of designing materials with selected properties simply by adjusting the composition of the oligomer precursor during the synthesis step. The tan δ temperatures of the prepared materials ranged from 31 to 93 °C, demonstrating the high tunability of the system.

Due to the associative character of the imine metathesis exchange mechanism adopted, the relaxation times followed an Arrhenius dependence with the temperature. This relationship allowed us to calculate the activation energies (between 28 and 85 kJ/mol) and the topology freezing transition temperature (T_v) between −53 and 86 °C. Since this temperature is lower than T_g, the materials must reach the latter temperature before being reshaped or recycled. Moreover, a linear correlation of E_a and T_v with respect to the concentration of exchangeable groups was found.

As a general trend, materials prepared with Jeffamine D-230 showed good creep resistance at 20 °C, while the creep deformation was higher in samples prepared with Jeffamine D-400. Thus, creep was strongly dependent on the content of PPO units in the network and the mobility of the chains formed.

Furthermore, the results evidenced that increasing the imine concentration simultaneously improves the creep resistance and the stress relaxation properties at 20 °C, while the reduction of the relaxation time is usually accompanied by a higher creep deformation.

An almost complete chemical degradation of these polyimine-based vitrimers could be achieved by tuning the material composition: the amount of DETA and Jeffamine employed; and the type of Jeffamine used, which also revealed the advantages of the synthetic strategy adopted in this research work.

CRediT authorship contribution statement

Tommaso Telatin: Writing – original draft, Validation, Methodology, Investigation, Formal analysis. **Silvia De la Flor:** Writing – review & editing, Validation, Resources, Funding acquisition, Formal analysis, Data curation, Conceptualization. **Àngels Serra:** Writing – review & editing, Validation, Supervision, Resources, Project administration, Funding acquisition, Formal analysis, Data curation, Conceptualization. **Xavier Montané:** Writing – review & editing, Validation, Supervision, Resources, Project administration, Formal analysis, Data curation, Conceptualization.

Declaration of competing interest

The authors declare that they have no known competing financial interests or personal relationships that could have appeared to influence the work reported in this paper.

Data availability

Data will be made available on request.

Acknowledgements

This work is part of the R&D projects PID2020-115102RB-C21 and TED2021-131102B–C22, funded by MCIN/AEI/10.13039/501100011033 and European Union NextGeneration EU/PRTR. Furthermore, this work was supported by the Generalitat de Catalunya, grant number 2021-SGR-00154.

Appendix A. Supplementary data

Supplementary data to this article can be found online at https://doi.org/10.1016/j.polymertesting.2024.108465.

References

[1] C.J. Kloxin, C.N. Bowman, Covalent adaptable networks: smart, reconfigurable and responsive network systems, Chem. Soc. Rev. 42 (2013) 7161–7173, https://doi.org/10.1039/C3CS60046G.

[2] J. Zheng, Z.M. Png, S.H. Ng, G.X. Tham, E. Ye, S.S. Goh, X.J. Loh, Z. Li, Vitrimers: current research trends and their emerging applications, Mater. Today 51 (2021) 568–625, https://doi.org/10.1016/j.mattod.2021.07.003.

[3] M. Podgórski, B.D. Fairbanks, B.E. Kirkpatrick, M. McBride, A. Martinez, A. Dobson, N.J. Bongiardina, C.N. Bowman, Toward stimuli-responsive dynamic thermosets through continuous development and improvements in Covalent Adaptable Networks (CANs), Adv. Mater. 32 (2020) 1906876, https://doi.org/10.1002/adma.201906876.

[4] L.E. Porath, C.M. Evans, Importance of broad temperature windows and multiple rheological approaches for probing viscoelasticity and entropic elasticity in vitrimers, Macromolecules 54 (2021) 4782–4791, https://doi.org/10.1021/acs.macromol.0c02800.

[5] L. Li, X. Chen, M.B. Rusayyis, K. Jin, J.M. Torkelson, Arresting elevated temperature creep and achieving full cross-link density recovery in reprocessable polymer networks and network composites via nitroxide-mediated dynamic chemistry, Macromolecules 54 (2021) 1452–1464, https://doi.org/10.1021/acs.macromol.0c01691.

[6] J.J. Lessard, G.M. Scheutz, S.H. Sung, K.A. Lantz, T.H. Epps III, B.S. Sumerlin, Block copolymer vitrimers, J. Am. Chem. Soc. 142 (2020) 283–289, https://doi.org/10.1021/jacs.9b10360.

[7] M.J. Webber, M.W. Tibbitt, Dynamic and reconfigurable materials from reversible network interactions, Nat. Rev. Mater. 7 (2022) 541–556, https://doi.org/10.1038/s41578-021-00412-x.

[8] F. Meng, M.O. Saed, E.M. Terentjev, Elasticity and relaxation in full and partial vitrimer networks, Macromolecules 52 (2019) 7423–7429, https://doi.org/10.1021/acs.macromol.9b01123.

[9] F. Ling, Z. Liu, M. Chen, H. Wang, Y. Zhu, C. Ma, J. Wu, G. Huang, Compatibility driven self-strengthening during the radical-responsive remolding process of polyisoprene vitrimers, J. Mater. Chem. A 7 (2019) 25324–25332, https://doi.org/10.1039/c9ta09292g.

[10] A. Jourdain, R. Asbai, O. Anaya, M.M. Chehimi, E. Drockenmuller, D. Montarnal, Rheological properties of Covalent Adaptable Networks with 1,2,3-triazolium cross-links: the missing link between vitrimers and dissociative networks, Macromolecules 53 (2020) 1884–1900, https://doi.org/10.1021/acs.macromol.9b02204.

[11] D. Montarnal, M. Capelot, F. Tournilhac, L. Leibler, Silica-like malleable materials from permanent organic networks, Science 334 (2011) 965–968, https://doi.org/10.1126/science.1212648.

[12] D.J. Fortman, R.L. Snyder, D.T. Sheppard, W.R. Dichtel, Rapidly reprocessable cross-linked polyhydroxyurethanes based on disulfide exchange, ACS Macro Lett. 7 (2018) 1226–1231, https://doi.org/10.1021/acsmacrolett.8b00667.

[13] S.-H. Lee, S.-R. Shin, D.-S. Lee, Self-healing of cross-linked PU via dual-dynamic covalent bonds of a Schiff base from cystine and vanillin, Mater. Des. 172 (2019) 107774, https://doi.org/10.1016/j.matdes.2019.107774.

[14] A. Roig, M. Agizza, À. Serra, S. De la Flor, Disulfide vitrimeric materials based on cystamine and diepoxy eugenol as bio-based monomers, Eur. Polym. J. 194 (2023) 112185, https://doi.org/10.1016/j.eurpolymj.2023.112185.

[15] M. Capelot, D. Montarnal, F. Torunilhac, L. Leibler, Metal-catalyzed transesterification for healing and assembling of thermosets, J. Am. Chem. Soc. 134 (2012) 7664–7667, https://doi.org/10.1021/ja302894k.

[16] F.I. Altuna, C.E. Hoppe, R.J.J. Williams, Shape memory epoxy vitrimers based on DGEBA crosslinked with dicarboxylic acids and their blends with citric acid, RSC Adv. 6 (2016) 88647–88655, https://doi.org/10.1039/C6RA18010H.

[17] F.I. Altuna, C.E. Hoppe, R.J.J. Williams, Epoxy vitrimers with covalently bonded tertiary amine as catalyst of the transesterification reaction, Eur. Polym. J. 113 (2019) 297–304, https://doi.org/10.1016/j.eurpolymj.2019.01.045.

[18] A. Roig, A. Petrauskaitė, X. Ramis, S. De la Flor, À. Serra, Synthesis and characterization of new bio-based poly-(acylhydrazone) vanillin vitrimers, Polym. Chem. 13 (2022) 1510–1519, https://doi.org/10.1039/D1PY01694F.

[19] M.E. Belowich, J.F. Stoddart, Dynamic imine chemistry, Chem. Soc. Rev. 41 (2012) 2003–2024, https://doi.org/10.1039/C2CS15305J.

[20] X. Zhang, S. Wang, Z. Jiang, Y. Li, X. Jing, Boronic ester based vitrimers with enhanced stability via internal boron-nitrogen coordination, J. Am. Chem. Soc. 142 (2020) 21852–21860, https://doi.org/10.1021/jacs.0c10244.

[21] Y. Chen, Z. Tang, X. Zhang, Y. Liu, S. Wu, B. Guo, Covalently cross-linked elastomers with self-healing and malleable abilities enabled by boronic ester bonds, ACS Appl. Mater. Interfaces 10 (2018) 24224–24231, https://doi.org/10.1021/acsami.8b09863.

[22] O.R. Cromwell, J. Chung, Z. Guan, Malleable and self-healing covalent polymer networks through tunable dynamic boronic ester bonds, J. Am. Chem. Soc. 137 (2015) 6492–6495, https://doi.org/10.1021/jacs.5b03551.

[23] W. Denissen, G. Rivero, R. Nicolaÿ, L. Leibler, J.M. Winne, F.E. Du Prez, Vinylogous urethane vitrimers, Adv. Funct. Mater. 25 (2015) 2451–2457, https://doi.org/10.1002/adfm.201404553.

[24] S. Engelen, A.A. Wróblewska, K. De Bruycker, R. Aksakal, V. Ladmiral, S. Caillol, F. E. Du Prez, Sustainable design of vanillin-based vitrimers using vinylogous urethane chemistry, Polym. Chem. 13 (2022) 2665–2673, https://doi.org/10.1039/D2PY00351A.

[25] M. Ciaccia, S. Di Stefano, Mechanisms of imine exchange reactions in organic solvents, Org. Biomol. Chem. 13 (2015) 646–654, https://doi.org/10.1039/C4OB02110J.

[26] P. Taynton, K. Yu, R.K. Shoemaker, Y. Jin, H.J. Qi, W. Zhang, Heat or water driven malleability in a highly recyclable covalent network polymer, Adv. Mater. 26 (2014) 3938–3942, https://doi.org/10.1002/adma.201400317.

[27] Y. Liu, F. Lu, N. Xu, B. Wang, L. Yang, Y. Huang, Z. Hu, Mechanically robust, hydrothermal aging resistant, imine-containing epoxy thermoset for recyclable carbon fiber reinforced composites, Mater. Des. 224 (2022) 111357, https://doi.org/10.1016/j.matdes.2022.111357.

[28] P. Taynton, C.P. Zhu, S. Loob, R. Shoemaker, J. Pritchard, Y.H. Jin, W. Zhang, Rehealable polyimine thermosets polymer composition and moisture sensitivity, Polym. Chem. 7 (2016) 7052–7056, https://doi.org/10.1039/C6PY01395C.

[29] J.M. Whiteley, P. Taynton, W. Zhang, S.H. Lee, Ultra-thin solid-state Li-ion electrolyte membrane facilitated by a self- healing polymer matrix, Adv. Mater. 27 (2015) 6922–6927, https://doi.org/10.1002/adma.201502636.

[30] P. Taynton, H.G. Ni, C.P. Zhu, K. Yu, S. Loob, Y.H. Jin, H.J. Qi, W. Zhang, Repairable woven carbon fiber composites with full recyclability enabled by malleable polyimine networks, Adv. Math. 28 (2016) 2904–2909, https://doi.org/10.1002/adma.201505245.

[31] H. Zheng, Q. Liu, X. Lei, Y. Chen, B. Zhang, Q. Zhang, Performance-modified polyimine vitrimers: flexibility, thermal stability and easy reprocessing, J. Mater. Sci. 54 (2019) 2690–2698, https://doi.org/10.1007/s10853-018-2962-4.

[32] X.L. Zhao, Y.Y. Liu, Y. Weng, Y.D. Li, J.B. Zeng, Sustainable epoxy vitrimers from epoxidized soybean oil and vanillin, ACS Sustainable Chem. Eng. 8 (2020) 15020–15029, https://doi.org/10.1021/acssuschemeng.0c05727.

[33] A. Roig, P. Hidalgo, X. Ramis, S. De la Flor, À. Serra, Vitrimeric epoxy-amine polyimine networks based on a renewable vanillin derivative, ACS Appl. Polym. Mater. 4 (12) (2022) 9341–9350, https://doi.org/10.1021/acsapm.2c01604.

[34] K. Liang, G. Zhang, J. Zhao, L. Shi, J. Cheng, J. Zhang, Malleable, recyclable, and robust poly(amide–imine) vitrimers prepared through a green polymerization process, ACS Sustain. Chem. Eng. 9 (2021) 5673–5683, https://doi.org/10.1021/acssuschemeng.1c00626.

[35] H. Liu, H. Zhang, H. Wang, X. Huang, G. Huang, J. Wu, Weldable, malleable and programmable epoxy vitrimers with high mechanical properties and water insensitivity, Chem. Eng. J. 368 (2019) 61–70, https://doi.org/10.1016/j.cej.2019.02.177.

[36] L. Li, X. Chen, K. Jin, J.M. Torkelson, Vitrimers designed both to strongly suppress creep and to recover original cross-link density after reprocessing: quantitative theory and experiments, Macromolecules 51 (2018) 5537–5546, https://doi.org/10.1021/acs.macromol.8b00922.

[37] M. Capelot, M.M. Unterlass, F. Tournilhac, L. Leibler, Catalytic control of the vitrimer glass transition, ACS Macro Lett. 1 (2012) 789–792, https://doi.org/10.1021/mz300239f.

[38] Z. Yang, Q. Wang, T. Wang, Dual-triggered and thermally reconfigurable shape memory graphene-vitrimer composites, ACS Appl. Mater. Interfaces 8 (2016) 21691–21699, https://doi.org/10.1021/acsami.6b07403.

[39] O. Konuray, X. Fernández-Francos, X. Ramis, Structural design of CANs with fine-tunable relaxation properties: a theoretical framework based on network structure and kinetics modeling, Macromolecules 56 (2023) 4855–4873, https://doi.org/10.1021/acs.macromol.3c00482.

[40] S.K. Schoustra, T. Groeneveld, M.M.J. Smulders, The effect of polarity on the molecular exchange dynamics in imine-based covalent adaptable networks, Polym. Chem. 12 (2021) 1635–1642, https://doi.org/10.1039/D0py01555e.

[41] K. Kimura, Chapter 5 - five-membered heterocycles, in: V.J. Ram, A. Sethi, M. Nath, R. Pratap (Eds.), The Chemistry of Heterocycles, Elsevier Science BV, Amsterdam, 2019, pp. 149–478, https://doi.org/10.1016/B978-0-08-101033-4.00005-X.

[42] K. Kimura, Nonstoichiometric polycondensation, in: K. Matyjaszewski, M. Möller (Eds.), Polymer Science: A Comprehensive Reference, vol. 5, Elsevier Science BV, Amsterdam, 2012, pp. 95–113, https://doi.org/10.1016/B978-0-444-53349-4.00133-3.

[43] Y. Spiesschaert, C. Taplan, L. Stricker, M. Guerre, J.M. Winne, F.E. Du Prez, Influence of the polymer matrix on the viscoelastic behaviour of vitrimers, Polym. Chem. 11 (2020) 5377–5385, https://doi.org/10.1039/D0PY00114G.

[44] P. Miao, X. Leng, J. Liu, G. Song, M. He, Y. Li, Regulating the dynamic behaviors of transcarbamoylation-based vitrimers via mono-variation in density of exchangeable hydroxyl, Macromolecules 55 (2022) 4956–4966, https://doi.org/10.1021/acs.macromol.2c00127.

[45] A.M. Hubbard, Y. Ren, C.R. Picu, A. Sarvestani, D. Konkolewicz, A.K. Roy, V. Varshney, D. Nepal, Creep mechanics of epoxy vitrimer materials, ACS Appl. Polym. Mater. 4 (2022) 4254–4263, https://doi.org/10.1021/acsapm.2c00230.

[46] Y. Liu, F. Lu, N. Xu, B. Wang, L. Yang, Y. Huang, Z. Hu, Mechanically robust, hydrothermal aging resistant, imine-containing epoxy thermoset for recyclable carbon fiber reinforced composites, Mater. Des. 224 (2022) 111357, https://doi.org/10.1016/j.matdes.2022.111357.